COMMUNICATION

Plasma-assisted electrochemical exfoliation of graphite for rapid production of graphene sheets†

Dang Van Thanh,[a] Lain-Jong Li,[b] Chih-Wei Chu,[c] Po-Jen Yen[a] and Kung-Hwa Wei*[a]

We describe a new and highly efficient plasma-assisted electrochemical exfoliation method, involving a plasma-generated graphite cathode and a graphite anode, for the production of graphene sheets from electrodes in a basic electrolyte solution in a short reaction time.

Graphene sheets (GSs), including graphite nanoplatelets (GNPs), graphite nanosheets (GNs), exfoliated graphite (EG), and multiple-layer graphene, are nanometer-scale platelets that comprise of a few layers of planar graphene with platelet thicknesses ranging from 0.34 to 100 nm.[1–3] Recently, GSs have attracted great interest because of their extraordinary properties and their potential applications in energy storage,[4] composites materials,[5] and polymer/GNP nanocomposites.[6] The methods through which GSs are synthesized determine their structures and, therefore, can influence their practical applications.[7–11] Several methods have been developed for the preparation of GSs, including chemical vapor deposition,[12] discharging,[13,14] mechanical milling,[15,16] liquid-phase exfoliation of graphite,[17,18] chemical reduction of exfoliated graphite oxide (GO),[19,20] and electrochemical exfoliation.[21–29] Among them, the electrochemical exfoliation of graphite is one of the simplest and most convenient methods for the large-scale production of GSs. Herein, we describe a highly efficient plasma-assisted electrochemical exfoliation method, involving a plasma-generated graphite cathode and a graphite anode, for the production of graphene sheets from electrodes in a basic electrolyte solution in a short reaction time.

In the present study, a much larger potential, 60 V, as compared to 5–10 V in the case of conventional electrochemical method, is applied to the high-purity graphite (HG) cathode that maintain its tip barely above the basic electrolyte, a solution containing a mixture of KOH and $(NH_4)_2SO_4$, different from conventional electrochemical cells,[22,26,30] while the rod-HG anode is submerged in the electrolyte. Because the surface contact area of cathode in the electrolyte is much smaller than that of the anode, an extremely high electric field is generated near the cathode surface that is in contact with the electrolyte. Simultaneously, hydrogen gas bubbles evolved from the hydrolysis of the water in the electrolyte near the surface contact area of the cathode tip. As a result of an instant ionization of hydrogen gas bubbles by the presence the high electric field near the cathode tip, the onset of plasma around the cathode tip takes place (see the demonstration movie in the ESI,† as well as the detailed experimental conditions).

Fig. 1a show a schematic representation of the equipment used for production of the plasma-electrochemically exfoliated graphene sheets (PEEG). Fig. 1b and c display images of the electrolyte at various times during the PEEG, revealing a change in color, from colorless to dark, after only 5 min (see movie in the ESI†), suggesting a high exfoliation rate when using this method. Fig. 1e displays a photograph of the PEEG dispersion
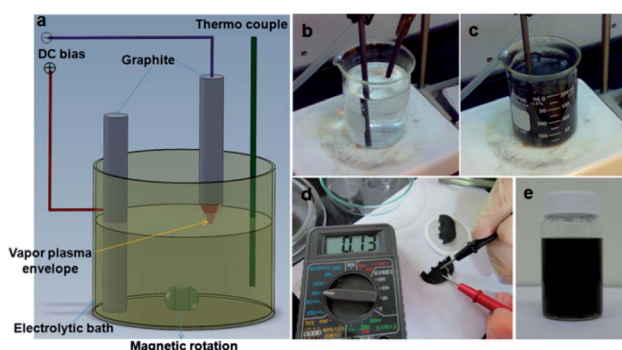

Fig. 1 (a) Schematic representation of the equipment used for PEEG. (b–e) Photographs of (b and c) the electrolytic solution (b) before and (c) after plasma-assisted electrochemical exfoliation process; (d) the PEEG-based graphene film prepared through vacuum filtering of the electrolyte after plasma-assisted electrochemical exfoliation process; and (e) a dispersion of PEEG in an NMP solution.

[a]Department of Material Science and Engineering, National Chiao Tung University, Hsinchu 300, Taiwan. E-mail: khwei@mail.nctu.edu.tw; Fax: +886-35-724-727
[b]Institute of Atomic and Molecular Sciences, Academia Sinica, Taipei, 11529, Taiwan
[c]Research Center for Applied Sciences, Academia Sinica, Taipei, 11529, Taiwan

in NMP after settling for 6 h; this sample exhibited good dispersion and homogeneity and was stable for a period of 72 h. In addition, the PEEG-based graphene film prepared through vacuum-filtering of the electrolyte after plasma-assisted electrochemical exfoliation process exhibited good conductive properties with resistance of 130 Ω (Fig. 1d) and sheet resistance of 121 Ω. per square area with a four-probe method. This graphene film might have been compressed during filtration, resulting in re-agglomeration of graphene nanosheets.

Fig. 2a displays X-ray diffraction (XRD) patterns of the HG and PEEG; that of the HG displays a characteristic sharp, high-intensity (002) peak at a value of 2θ of 26.6° and three small peaks at values of 2θ of 42.8, 44.6, and 54.6°, corresponding to the 100, 101, and 004 reflections, respectively. After the HG had experienced plasma-assisted electrochemical exfoliation process, the intensity of the characteristic (002) peak at 26.6° decreased significantly, suggesting that the graphitic lattice of HG had changed its periodic arrangement in the z-direction after exfoliation into graphite flakes. Additionally, the Raman spectra of HG and PEEG (Fig. 2b) reveal a structural change from HG to PEEG. The Raman spectrum of HG features a weak D (defect) band, a prominent G (graphite) band, and a broad 2D (doubly generated G) band at 1353, 1579, and 2706 cm^{-1}, respectively, which are characteristic bands of graphite.[31,32] In the Raman spectrum of PEEG, the G band was broader and had shifted to a lower frequency and the D band was more pronounced than that in the spectrum of HG, implying that defects or structural disorder had occurred in the graphitic lattice of PEEG. Notably, the 2D band of PEEG had shifted to a lower frequency with a significant increase in intensity relative to that of HG, indicating the formation of graphene structures in PEEG. [18,25,33–35]

Fig. 2c displays the C 1s XPS spectrum of HG; we de-convoluted the C 1s XPS signal into one major peak at 284.4 eV representing C=C bonds (sp^2-hybridized carbon atoms) and a minor peak at 285.5 eV representing C–C bonds (sp^3-hybridized carbon atoms).[36] Fig. 2d presents the C 1s XPS spectrum for PEEG; we could de-convolute it into three peaks: the signals of PEEG at binding energies of 284.4 and 285.5 eV represent non-oxygenated carbon components—C=C (sp^2-hybridized carbon atoms) and C–C (sp^3-hybridized carbon atoms) bonds, respectively—while the other at 286.4 eV represents oxygenated C–O components (i.e., hydroxyl and epoxy units). The intensity and sharpness of the graphitic C=C/C–C signals decreased and widened significantly relative to those of the HG sample, implying that some oxygen-containing functional groups had attacked the C=C bonds in the graphite to generate C–O bonds, resulting in their partial oxidation.[36,37] Fig. 3a–d present SEM and TEM images of the aggregated PEEG samples that were collected after filtration with PVDF film and dispersed in NMP, respectively; they indicate a dramatic change in morphology in the prepared samples. The HG comprised thick, bulk graphite flakes that transformed into thinner nanometer-scale platelets after plasma-assisted electrochemical exfoliation process. We also observed scrolled graphene sheets, as indicates by the arrows in S2 and S3 in the ESI,† where in the folded regions, the thickness of layers could be approximately determined (see
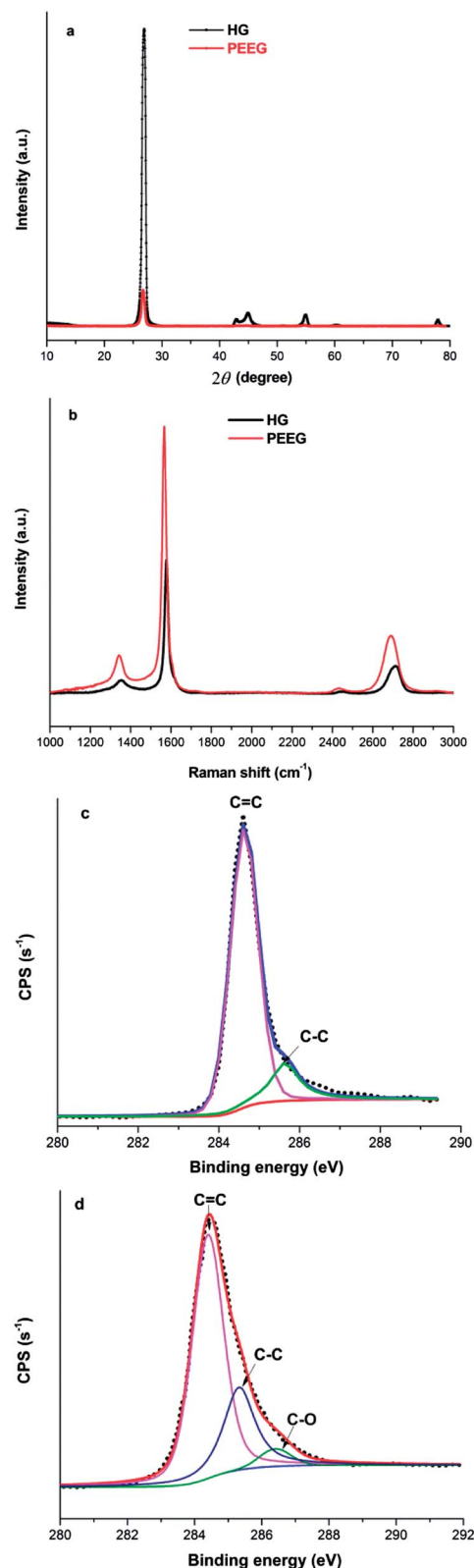

Fig. 2 (a) XRD patterns of HG and PEEG. (b) Raman spectra of HG and PEEG. (c) XPS spectra (C 1s signal) of HG. (d) XPS spectra (C 1s signal) of PEEG.
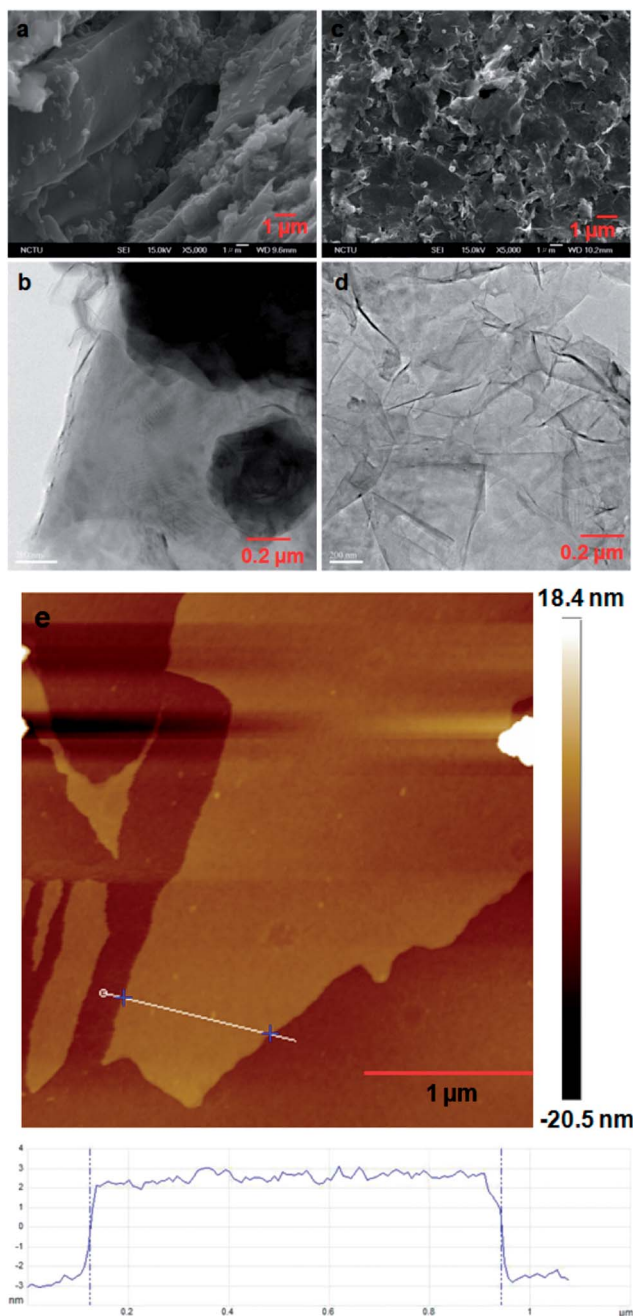
Fig. 3   (a and c) SEM and (b and d) TEM images of (a and b) HG and (c and d) PEEG. (e) AFM image and height profile of a PEEG sample deposited on a Si/SiO$_2$ substrate.

based on an interlayer spacing of 0.34 nm, confirming the formation of graphene sheets. The exfoliated graphite flakes have a tendency to aggregate and stack on each other after drying on the surface of Si/SiO$_2$ substrate and copper grid when they are used for SEM and TEM observation, resulting in different thickness values obtained using SEM/TEM and AFM imaging.

Table S2† displays a comparison between the PEEG that were produced with the plasma-assisted electrochemical method and a conventional electrochemical method and indicates the production rate of graphene sheets is six times as fast as that obtained from the conventional electrochemical method, 32 mg *vs.* 5 mg in five minutes. Moreover, the PEEG produced are larger and thinner than that fabricated by the conventional electrochemical method (see S4 and S5 in ESI†), suggesting that the plasma-assisted electrochemical exfoliation method appears to be a very efficient means of synthesizing graphene sheets.

Fig. 4 depicts the mechanism of the formation of graphene sheets from graphite. We suspect that rapid hydrogen bubble evolution (hydrolysis of water) in the cathode played a role in the exfoliation of the graphite as depicted in Fig. 4: first, a violent release of hydrogen gas on the tip of the HG surface cathode results in opened up the edge sheets of the its surface and facilitated the intercalation of hydrogen gas into the graphite layers, forming graphite intercalation compounds, as a result of these expansion processes, the van der Waals forces between the graphitic sheets weakened. Second, in the plasma the temperature could instantaneously reach above 2000 °C within a short period of time (*e.g.*, <10^{-6} s)[38] on the HG tip surface during discharging, thermo-mechanical stresses occurred on this surface. A combination of these two factors induces the expansion and sequential exfoliation of the surface layer of the thick graphite cathode into smaller and thinner graphene sheets. Furthermore, electrochemical reactions on the surface of anode could induce exfoliation directly from graphite electrode, producing a small portion of graphene sheets from the starting graphite. Thus, our method is a new route toward the production of graphene sheets from both electrodes simultaneously in a basic electrolyte medium.

In conclusion, graphene sheets with good dispersion in solvents can be prepared through plasma-assisted electro-chemical exfoliation process at moderate temperatures without the need for acidic media. This method is quite promising because of its simple setup, environmentally benign, and rapid throughput.

high-magnification images of the folded regions in S2 and S3 in ESI†). SEM and TEM image analyses on aggregated PEEG sheets revealed that the average lateral dimensions was approximately 2.5 μm with a thickness of approximately 10–30 nm, which is close to the dimensions of a nanoplatelet, based on cross-sectional imaging of the folded edges of PEEG after tilting the sample from 0 to 25°; furthermore, Fig. 3e show the AFM image of the samples prepared from a diluted solution, revealing an average lateral dimensions of approximately 2.5 μm and a thickness of approximately 2.5 nm for an individual graphene sheet, corresponding to approximately seven layers of graphene,

Fig. 4   Proposed mechanisms for the formation of PEEG.

Acknowledgements

Notes and references

1 S. Stankovich, D. A. Dikin, R. D. Piner, K. A. Kohlhaas, A. Kleinhammes, Y. Jia, Y. Wu, S. T. Nguyen and R. S. Ruoff, *Carbon*, 2007, **45**, 1558.

2 J. Shen, Y. Hu, M. Shi, X. Lu, C. Qin, C. Li and M. Ye, *Chem. Mater.*, 2009, **21**, 3514.

3 L. Chen, Y. Hernandez, X. Feng and K. Müllen, *Angew. Chem., Int. Ed.*, 2012, **51**, 7640.

4 M. Pumera, *Energy Environ. Sci.*, 2011, **4**, 668.

5 D. Vuluga, J.-M. Thomassin, I. Molenberg, I. Huynen, B. Gilbert, C. Jerome, M. Alexandre and C. Detrembleur, *Chem. Commun.*, 2011, **47**, 2544.

6 C. Wu, X. Huang, G. Wang, L. Lv, G. Chen, G. Li and P. Jiang, *Adv. Funct. Mater.*, 2013, **23**, 506.

7 D. A. C. Brownson and C. E. Banks, *Chem. Commun.*, 2012, **48**, 1425.

8 K. M. F. Shahil and A. A. Balandin, *Nano Lett.*, 2012, **12**, 861.

9 F. He, S. Lau, H. L. Chan and J. Fan, *Adv. Mater.*, 2009, **21**, 710.

10 J.-Y. Kim, W. H. Lee, J. W. Suk, J. R. Potts, H. Chou, I. N. Kholmanov, R. D. Piner, J. Lee, D. Akinwande and R. S. Ruoff, *Adv. Mater.*, 2013, **16**, 2308.

11 Y. Xue, J. Liu, H. Chen, R. Wang, D. Li, J. Qu and L. Dai, *Angew. Chem., Int. Ed.*, 2012, **51**, 12124.

12 C.-T. Lin, P. T. K. Loan, T.-Y. Chen, K.-K. Liu, C.-H. Chen, K.-H. Wei and L.-J. Li, *Adv. Funct. Mater.*, 2013, **23**, 2301.

13 H. Fan, L. Wang, K. Zhao, N. Li, Z. Shi, Z. Ge and Z. Jin, *Biomacromolecules*, 2010, **11**, 2345.

14 Y. Wu, B. Wang, Y. Ma, Y. Huang, N. Li, F. Zhang and Y. Chen, *Nano Res.*, 2010, **3**, 661.

15 C. Knieke, A. Berger, M. Voigt, R. N. K. Taylor, J. Röhrl and W. Peukert, *Carbon*, 2010, **48**, 3196.

16 M. V. Antisari, A. Montone, N. Jovic, E. Piscopiello, C. Alvani and L. Pilloni, *Scr. Mater.*, 2006, **55**, 1047.

17 E.-K. Choi, I.-Y. Jeon, S.-Y. Bae, H.-J. Lee, H. S. Shin, L. Dai and J.-B. Baek, *Chem. Commun.*, 2010, **46**, 6320.

18 J. Geng, B.-S. Kong, S. B. Yang and H.-T. Jung, *Chem. Commun.*, 2010, **46**, 5091.

19 H.-J. Shin, K. K. Kim, A. Benayad, S.-M. Yoon, H. K. Park, I.-S. Jung, M. H. Jin, H.-K. Jeong, J. M. Kim, J.-Y. Choi and Y. H. Lee, *Adv. Funct. Mater.*, 2009, **19**, 1987.

20 O. C. Compton, B. Jain, D. A. Dikin, A. Abouimrane, K. Amine and S. T. Nguyen, *ACS Nano*, 2011, **5**, 4380.

21 J. Wang, K. K. Manga, Q. Bao and K. P. Loh, *J. Am. Chem. Soc.*, 2011, **133**, 8888.

22 K. Parvez, R. Li, S. R. Puniredd, Y. Hernandez, F. Hinkel, S. Wang, X. Feng and K. Müllen, *ACS Nano*, 2013, **7**, 3598.

23 D. Wei, L. Grande, V. Chundi, R. White, C. Bower, P. Andrew and T. Ryhanen, *Chem. Commun.*, 2012, **48**, 1239.

24 M. Zhou, J. Tang, Q. Cheng, G. Xu, P. Cui and L.-C. Qin, *Chem. Phys. Lett.*, 2013, **572**, 61.

25 T. Lin, J. Chen, H. Bi, D. Wan, F. Huang, X. Xie and M. Jiang, *J. Mater. Chem. A*, 2013, **1**, 500.

26 C. T. J. Low, F. C. Walsh, M. H. Chakrabarti, M. A. Hashim and M. A. Hussain, *Carbon*, 2013, **54**, 1.

27 D. A. C. Brownson, D. K. Kampouris and C. E. Banks, *Chem. Soc. Rev.*, 2012, **41**, 6944.

28 B. Erable, N. Duteanu, S. M. S. Kumar, Y. Feng, M. M. Ghangrekar and K. Scott, *Electrochem. Commun.*, 2009, **11**, 1547.

29 M. Mao, M. Wang, J. Hu, G. Lei, S. Chen and H. Liu, *Chem. Commun.*, 2013, **49**, 5301.

30 C.-Y. Su, A.-Y. Lu, Y. Xu, F.-R. Chen, A. N. Khlobystov and L.-J. Li, *ACS Nano*, 2011, **5**, 2332.

31 A. C. Ferrari, J. C. Meyer, V. Scardaci, C. Casiraghi, M. Lazzeri, F. Mauri, S. Piscanec, D. Jiang, K. S. Novoselov, S. Roth and A. K. Geim, *Phys. Rev. Lett.*, 2006, **97**, 187401.

32 F. Tuinstra and J. L. Koenig, *J. Chem. Phys.*, 1970, **53**, 1126.

33 N. Liu, F. Luo, H. Wu, Y. Liu, C. Zhang and J. Chen, *Adv. Funct. Mater.*, 2008, **18**, 1518.

34 F. Zeng, Z. Sun, X. Sang, D. Diamond, K. T. Lau, X. Liu and D. S. Su, *ChemSusChem*, 2011, **4**, 1587.

35 L. M. Malard, M. A. Pimenta, G. Dresselhaus and M. S. Dresselhaus, *Phys. Rep.*, 2009, **473**, 51.

36 H.-K. Jeong, Y. P. Lee, R. J. W. E. Lahaye, M.-H. Park, K. H. An, I. J. Kim, C.-W. Yang, C. Y. Park, R. S. Ruoff and Y. H. Lee, *J. Am. Chem. Soc.*, 2008, **130**, 1362.

37 D. V. Thanh, H.-C. Chen, L.-J. Li, C.-W. Chu and K.-H. Wei, *RSC Adv.*, 2013, **3**, 17402.

38 A. L. Yerokhin, X. Nie, A. Leyland, A. Matthews and S. J. Dowey, *Surf. Coat. Technol.*, 1999, **122**, 73.